Journal of Applied Electrochemistry (2006) 36:395–402
DOI 10.1007/s10800-005-9094-7

Corrosion inhibition of carbon steel in acid chloride solution using ethoxylated fatty alkyl amine surfactants

M.A. MIGAHED[1,3,*], M. ABD-EL-RAOUF[1], A.M. AL-SABAGH[1] and H.M. ABD-EL-BARY[2]
[1]*Egyptian Petroleum Research Institute (EPRI), Nasr city, Cairo 11727, Egypt*
[2]*Al-Azhar University, Nasr city, Cairo, Egypt*
[3]*Department of General and Analytical Chemistry, University of Science and Technology (AGH-UST), ul. Reymonta 23, 30-059 Kraków, Poland*
*(*author for correspondence, e-mail: mohamedatiyya707@hotmail.com)*

Received 18 February 2005; accepted in revised form 18 October 2005

Key words: corrosion, carbon steel, non-ionic surfactants, potentiostatic polarisation, surface tension and activation energy

Abstract

Four novel non-ionic ethoxylated fatty alkyl amine surfactants (I–IV) were synthesised and investigated as corrosion inhibitors of carbon steel in 1 M hydrochloric acid solution using gravimetric, open circuit potential and potentiostatic polarisation techniques. The percentage inhibition efficiency (η%) for each inhibitor increased with increasing concentration until the critical micelle concentration (cmc) was reached. The maximum inhibition efficiency approached 95.1% in the presence of 400 ppm of the inhibitor (IV). It was found that the adsorption of the surfactants on carbon steel followed the Langmuir adsorption isotherm. Potentiostatic polarisation data indicated that these surfactants act as mixed type inhibitors. The values of activation energy (E_a*) of carbon steel dissolution in 1 M HCl were calculated in the absence and presence of 400 ppm of each inhibitor. Finally, scanning electron microscopy (SEM) was used to examine the surface morphology of polished carbon steel surfaces and those immersed in 1 M HCl in the absence and presence of 400 ppm of inhibitor (IV).

1. Introduction

In most oil production wells, chloride salts are found either dissolved in water or emulsified in crude. Salts also originate from brines injected for secondary recovery or from sea water ballast in marine tankers. Typically, the salts in crude oil consist of 75% NaCl, 15% $MgCl_2$ and 10% $CaCl_2$. When crude oils are loaded into distillation units and heated up to about 120 °C, hydrogen chloride gas is evolved as a product of $MgCl_2$ and $CaCl_2$ hydrolysis, while NaCl is essentially stable. Dry hydrogen chloride, especially in the presence of large amounts of hydrocarbon vapour or liquid is not corrosive to carbon steel, but when steam is settled down to the bottom of the crude tower and in the overhead condensing system, severe aqueous chloride corrosion of carbon steel occurs [1]. To counteract this, corrosion inhibitors must be injected continuously through the system [2]. The inhibition of steel corrosion in acidic media using surface active agents (surfactants) has been achieved by many workers [3–13]. The present work aimed to study the adsorption properties and the inhibitive effects of environmental friendly ethoxylated fatty alkyl amine surfactants on the corrosion rate of carbon steel in 1 M hydrochloric acid solution by both chemical and electrochemical techniques.

2. Experimental

2.1. *Chemical composition of carbon steel alloy*

Carbon steel alloy specimens were cut from unused petroleum pipeline as regular edged cuboids with dimension 3× 2 × 0.7 cm. The alloy had the following weight percentage chemical composition: 0.17 C, 0.008 S, 1.18 Mn, 0.008 P, 0.27 Si, 0.04 Ni, 0.04 Cr, 0.04 Mo and the remainder was iron.

2.2. *Synthesis of ethoxylated fatty alkyl amine surfactants*

Four ethoxylated fatty alkyl amine surfactants were synthesised according to the proportions illustrated in Table 1.

The following describes a typical procedure used for synthesis of the different ethoxylated fatty alkyl amine surfactants under study. The aliphatic amine was

Table 1. List of the synthesised surfactants includes, code number, name, structure and the number of ethylene oxide units

Code number of the inhibitor	Name and abbreviation	Structure	Number of ethylene oxide units
(I)	Decylamine ethoxylate (DAE_2)	$C_{10}H_{21}N[(CH_2CH_2O)H]_2$	2
(II)	Decylamine ethoxylate (DAE_{10})	$C_{10}H_{21}N[(CH_2CH_2O)_5H]_2$	10
(III)	Decylamine ethoxylate (DAE_{20})	$C_{10}H_{21}N[(CH_2CH_2O)_{10}H]_2$	20
(IV)	Hexadecylamine ethoxylate ($HDAE_{20}$)	$C_{16}H_{33}N[(CH_2CH_2O)_{10}H]_2$	20

charged into the reaction vessel with 0.3 g sodium metal as a catalyst and heated with continuous stirring while passing a stream of nitrogen gas through the system for 10 min. The nitrogen stream was then replaced by ethylene oxide at a rate which was regulated by monitoring the Hg level of the manometer. The ethoxylation process may be represented by the following general equation [14].

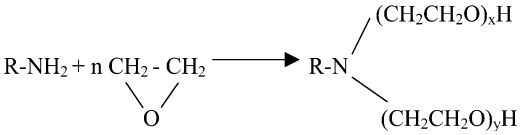

(1)

where, R = alky/chain

$x + y$ = number of ethylene oxide units

The chemical structure of the obtained compounds was confirmed by elemental analysis, FTIR and NMR techniques.

2.3. *Corrosion measurement*

The electrochemical measurements were carried out using a laboratory potentiostat (Wenking, LB 81M, Germany). The glass electrochemical cell was similar to that described by Greene [15]. Platinum was used as auxiliary electrode. All potentials were measured against a saturated calomel electrode (SCE) as reference.

The potentials of carbon steel electrodes were measured against the saturated calomel electrode in 1 M HCl solution in the absence and presence of different inhibitor concentrations. All measurements were carried out using a DM 301 Multi-tester, (Korea).

The specimens were polished with different grade emery papers, degreased with hot acetone [16]. Then washed with bi-distilled water and finally dried. The weight losses (mg cm^{-2}) of rectangular carbon steel specimens in 1 M HCl solution in the absence and presence of various concentrations of the inhibitors were determined. Triplicate specimens were exposed to each condition and the mean weight losses was reported.

The surface tension (γ) was measured using a Du-Nouy Tensiometer, (Kruss Type 8451) for various surfactants concentrations.

The surface morphology of each carbon steel specimen was examined using scanning electron microscopy (Jeol 5400, Japan). The energy of the acceleration beam employed was 30 kV.

3. Results and discussion

3.1. *Potentiostatic polarisation measurements*

Representative results are shown in Figure 1 for the inhibitor (IV). Electrochemical parameters such as corrosion potential (E_{corr}), corrosion current density (I_{corr}), cathodic and anodic Tafel slopes (b_c and b_a) and polarisation resistance (R_p) were calculated. The degree of surface coverage (θ) and the percentage inhibition efficiency ($\eta\%$) were calculated using the following equations [17]:

$$\theta = 1 - I/I_0 \tag{2}$$

$$\eta\% = \left[(I_0 - I)/I_0\right] \times 100 \tag{3}$$

where I_0 and I are the corrosion current densities in the absence and presence of the inhibitor, respectively.

The values of polarisation resistance (R_p) were calculated from the well known Stern–Geary equation [18]:

$$R_p = \frac{b_a b_c}{2.303 I_{corr}(b_a + b_c)} \tag{4}$$

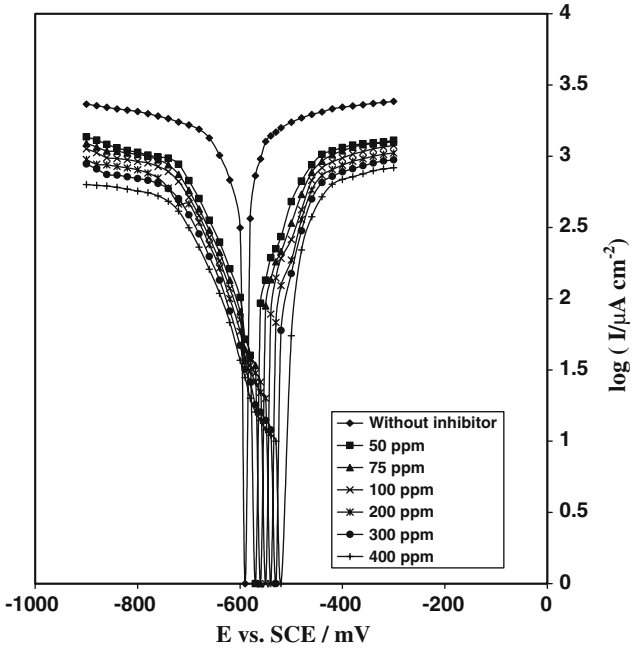

Fig. 1. Potentiostatic polarisaton curves of carbon steel in 1 M HCl in the absence and presence of different concentrations of the inhibitor (IV).

The results from potentiostatic polarisation measurements are summarised in Table 2 for inhibitors (I–IV). From these data it can be concluded that:

1. The Tafel lines are shifted to more negative and more positive potentials for the cathodic and anodic processes, respectively relative to the blank curve. This means that the selected surfactants act as mixed type inhibitors.
2. The slopes of the cathodic and anodic Tafel lines are approximately constant and independent of inhibitor concentration. This means that, the inhibitors have no effect on the metal dissolution mechanism.

From the results shown in Table 2, it is clear that at the same inhibitor concentration, the percentage inhibition efficiency ($\eta\%$) decreases in the following order: IV > III > II > I. This means that the effectiveness of the selected surfactants as corrosion inhibitors is increased by increasing both the number of ethylene oxide units and the alkyl chain length.

3.2. *Open circuit potential measurements*

The variation of the open circuit potentials of carbon steel electrodes as a function of exposure time were measured. Figure 2 shows the potential time curves in the absence and presence of different concentrations of inhibitor (IV). The corrosion potential (E_{corr}) in 1 M HCl (blank curve) tends, from the moment of immersion, towards more negative values. This behavior represents the break down of the pre-immersion, air formed, oxide film on the carbon steel surface. The electrode potential then shifts to more positive values until the steady state potential is established. The results indicated that, as the inhibitor concentration increases, the shift in (E_{corr}) was increased in the passive direction [19].

3.3. *Weight loss measurements*

Figure 3 shows the weight loss vs. time curves of carbon steel in 1 M HCl solution in the absence and presence of different concentrations of the inhibitor (IV). The weight loss of carbon steel decreases with increasing inhibitor concentration.

The degree of surface coverage (θ), the percentage inhibition efficiency ($\eta\%$) and the corrosion rate (k) of carbon steel were calculated from the following equations:

$$\theta = I - \frac{W}{W_0} \tag{5}$$

$$\eta\% = \left[(W_0 - W)/W_0\right] \times 100 \tag{6}$$

$$k = \frac{\text{weight loss, (mg cm}^{-2})}{\text{time, (hour)}} \tag{7}$$

where W_0 and W are the weight losses of the test specimens in the absence and presence of inhibitor.

Values obtained from weight loss measurements are summarised in Table 3 for the inhibitors (I–IV). It was found that, the percentage inhibition efficiency ($\eta\%$) decreases in the following order: IV > III > II > I. These

Table 2. Data obtained from potentiostatic polarisation of carbon steel in 1 M HCl solution in the absence and presence of various inhibitor concentrations at 303 K

Inhibitor	Conc./ppm	E_{corr}/mV	I_{corr}/μA cm^{-2}	b_c/mV dec^{-1}	b_a/mV dec^{-1}	$R_p/k\Omega$ cm^2	θ	$\eta\%$
1 M HCl (without inhibitor)	–	591	189.25	205	139	0.181	–	–
(I)	50	580	19.72	196	131	0.427	0.597	59.7
	75	577	65.55	194	131	0.518	0.669	66.9
	100	558	47.82	193	129	0.702	0.758	75.8
	200	546	41.96	193	129	0.800	0.788	78.8
	300	538	33.45	192	128	0.996	0.831	83.1
	400	530	29.30	192	128	1.140	0.852	85.2
(II)	50	579	70.65	201	134	0.494	0.643	64.3
	75	575	57.05	199	131	0.601	0.712	71.2
	100	554	40.82	199	131	0.840	0.794	79.4
	200	542	35.54	200	132	0.971	0.820	82.0
	300	535	27.10	200	133	1.279	0.863	86.3
	400	525	21.20	200	133	1.636	0.893	89.3
(III)	50	575	66.50	202	136	0.531	0.664	66.4
	156	570	50.60	200	135	0.692	0.744	74.4
	100	548	38.50	198	134	0.901	0.805	80.5
	200	536	28.15	200	135	1.243	0.858	85.8
	300	532	24.66	201	135	1.422	0.875	87.5
	400	522	17.90	202	134	1.954	0.909	90.9
(IV)	50	568	54.96	204	137	0.647	0.722	72.2
	75	563	42.68	202	136	0.827	0.784	78.4
	100	543	32.15	198	136	1.088	0.837	83.7
	200	530	23.45	200	137	1.505	0.881	88.1
	300	524	19.20	203	137	1.850	0.903	90.3
	400	515	13.75	204	138	2.599	0.930	93.0

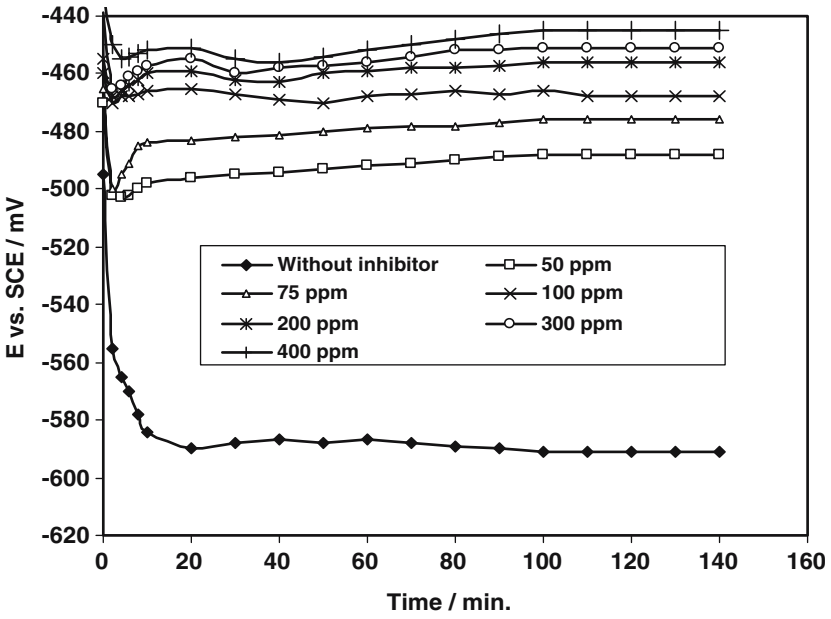

Fig. 2. Potential-Time curves for carbon steel in 1 M HCl in the absence and presence of different concentrations of the inhibitor (IV) at 303 K.

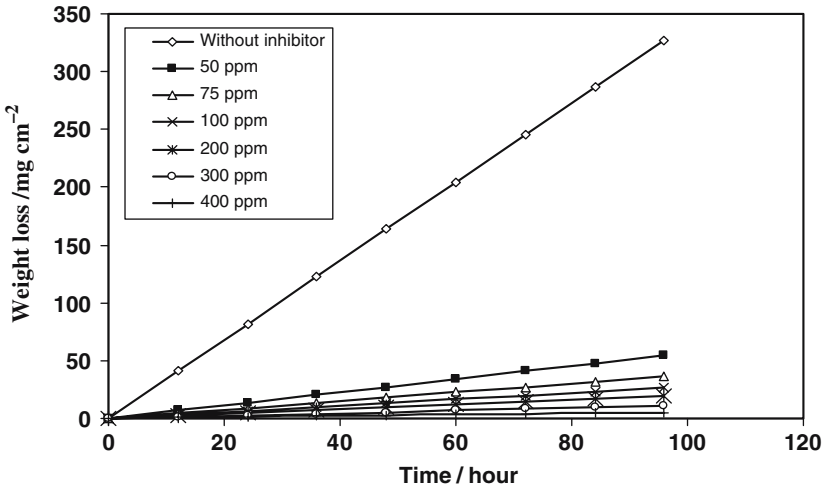

Fig. 3. Weight loss-time curves for carbon steel dissolution in 1 M HCl solution in absence and presence of different concentration of the inhibitor (IV) at 303 K.

results are in good agreement with that obtained from potentiostatic polarisation measurements.

Figure 4 illustrates the relationship between C_i/θ against C_i for the inhibitor (IV).The experimental results give a straight line with unit slope suggesting that the adsorption of the inhibitor molecules at the carbon steel/solution interface obeys the Langmuir adsorption isotherm, which is represented by the following equation:

$$C_i/\theta = 1/K_{ads} + C_i \quad (8)$$

where, C_i is the concentration of the inhibitor and K_{ads} represents the adsorption equilibrium constant. The relatively high value of K_{ads} (1.85×10^5) reflects the high adsorption ability of this inhibitor on carbon steel. It was found that the adsorption depends on the structure of the inhibitor molecule, the composition of the electrolyte, temperature, the nature of metal surface and the potential at the metal/solution interface [20].

3.4. *Effect of temperature*

The effect of temperature on the corrosion rate of carbon steel in 1 M HCl solution in the absence and presence of 400 ppm inhibitor (I–IV) was studied by the weight loss technique. The results indicate that the corrosion rate increases with increasing temperature in both the absence and presence of the inhibitors. Arrhenius plots of ($\log k$) against ($1/T$) for carbon steel dissolution in 1 M HCl solution in the absence and presence of 400 ppm inhibitor (IV) are shown in Figure 5.

Table 3. Data obtained from weight loss measurements for carbon steel dissolution in 1 M HCl solution in absence and presence of various inhibitor concentrations at 303 K

Inhibitor	Conc./ppm	Corrosion rate, 10^3 k /mg cm^{-2} h^{-1}	θ	η%
1 M HCl (without inhibitor)	–	31.1	–	–
(I)	50	9.4	0.697	69.7
	75	6.6	0.787	78.7
	100	3.7	0.881	88.1
	200	3.3	0.893	89.3
	300	2.7	0.913	91.3
	400	1.6	0.948	94.8
(II)	50	8.5	0.726	72.6
	75	5.6	0.819	81.9
	100	2.9	0.906	90.6
	200	2.3	0.926	92.6
	300	1.7	0.945	94.5
	400	1.5	0.951	95.1
(III)	50	6.6	0.786	78.6
	75	4.7	0.848	84.8
	100	2.8	0.904	90.9
	200	1.9	0.936	93.6
	300	1.4	0.955	95.5
	400	1.3	0.958	95.8
(IV)	50	5.6	0.819	81.9
	75	3.7	0.881	88.1
	100	2.6	0.916	91.6
	200	1.7	0.945	94.5
	300	1.2	0.961	96.1
	400	1.1	0.964	96.4

From the slopes of the plots, the respective activation energies (E_a*) were calculated from the following equation:

$$\log k = \frac{-E_a^*}{2.303R} \times \frac{1}{T} + \text{const.} \quad (9)$$

Detailed results are summarised in Table 4. The presence of the inhibitor increases the activation energy (E_a*) of carbon steel dissolution in 1 M HCl, hence the process is activation controlled [21]. The values of activation energy (E_a*) for the selected inhibitors decreased in the following order: IV > III > II > I, which is consistent with the stated results.

3.5. *Surface tension measurements*

The values of surface tension (γ) of the inhibitors (I-IV) were measured at various concentrations. The relationship between (γ) and ($\ln C$) for the inhibitor (IV) is shown in Figure 6. The intercept of the two lines designates the critical micelle concentration (cmc). The plot indicates that the surfactant is molecularly dispersed at low concentration leading to a reduction in surface tension (γ). This reduction in surface tension increases with increasing concentration. At higher concentration, however, when a certain concentration is reached (cmc), the surfactant molecules form micelles, which are in equilibrium with the free surfactant molecules [22]. Figure 7 shows the schematic representation of the molecular orientation on the positively charged carbon steel surface [23].

3.6. *Scanning electron microscopy*

Figure 8a shows a characteristic inclusion observed on the polished carbon steel surface, which was probably an oxide inclusion [24]. Figure 8b shows the SEM image of the surface of a carbon steel specimen after immersion in 1 M HCl solution for 5 days in the absence of inhibitor, while Figure 8c shows another carbon steel specimen after immersion in 1 M HCl solution to the same time interval in the presence of 400 ppm of the inhibitor (IV). The surface was corroded in the absence of inhibitor, but when 400 ppm of the inhibitor (IV) was added, there is a well inhibited surface. It is clear that inhibitor (IV) provides a good protective surface film. This explains the higher value of percentage inhibition efficiency (η%) obtained in the presence of 400 ppm of inhibitor (IV).

3.7. *Corrosion inhibition mechanism*

The inhibition effect by surfactants is attributed to the adsorption of the surfactant molecules via their functional group onto the metal surface. The adsorption rate is usually rapid and hence the reactive metal is shielded from the aggressive environment [25]. Corrosion inhibition depends on the adsorption ability on the corroding

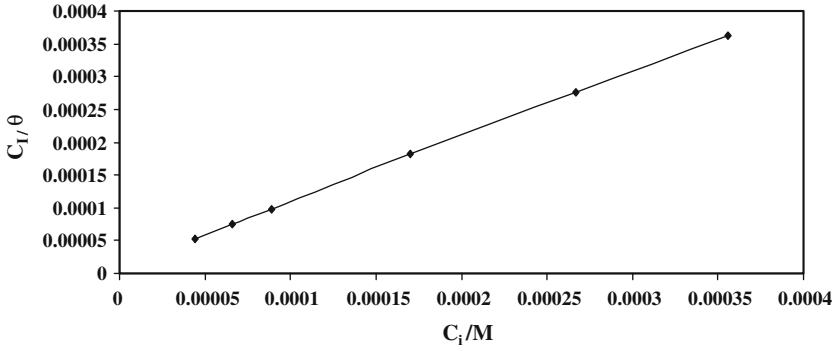

Fig. 4. Langmiur adsorption isotherm (C_i/θ vs. C_i) for the inhibitor (IV) on carbon steel surface in 1 M HCl at 303 K.

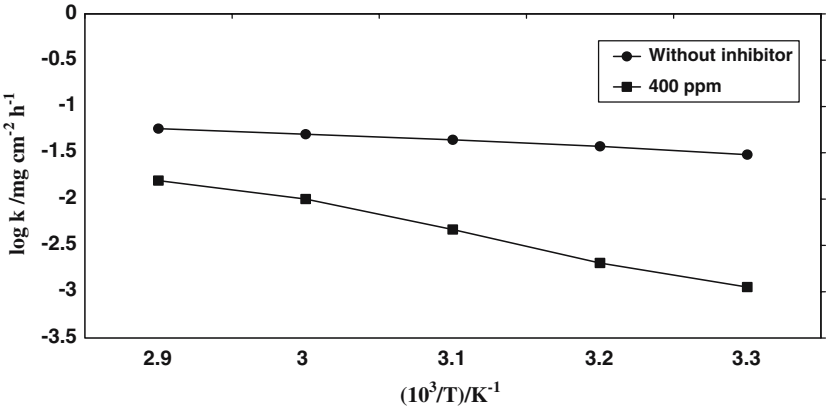

Fig. 5. Effect of temperature on the corrosion rate of carbon steel in 1 M HCl solution in the absence and presence of 400 ppm of the inhibitor (IV).

Table 4. Effect of temperature on the corrosion rate (k) of carbon steel in the absence and presence of 400 ppm inhibitors (I–IV)

Inhibitor	Temperature/K	Weight loss /mg cm^{-2} $\times 10^{-2}$	Corrosion rate, 10^3k /mg cm^{-2} h^{-1}	$(10^3\frac{1}{T})/k-1$	E_a* /kJ mol^{-1}
1 M HCl	303	45	30	3.3	30.39
(without inhibitor)	313	55	36	3.2	
	323	65	43	3.1	
	333	15	50	3.0	
	343	85	55	2.9	
(I)	303	2.5	1.6	3.3	45.95
	313	4.5	3.0	3.2	
	323	10	6.6	3.1	
	333	20	13.3	3.0	
	343	30	20.0	2.9	
(II)	303	2.2	1.5	3.3	47.80
	313	4.5	2.6	3.2	
	323	9.5	6.3	3.1	
	333	18.5	12.3	3.0	
	343	26.5	17.6	2.9	
(III)	303	2.0	1.3	3.3	49.78
	313	3.7	2.5	3.2	
	323	7.5	5.0	3.1	
	333	15.5	10.3	3.0	
	343	25.0	16.6	2.9	
(IV)	303	1.7	1.1	3.3	51.69
	313	3.1	2.3	3.2	
	323	5.0	3.3	3.1	
	333	12.5	8.0	3.0	
	343	23.5	15.6	2.9	

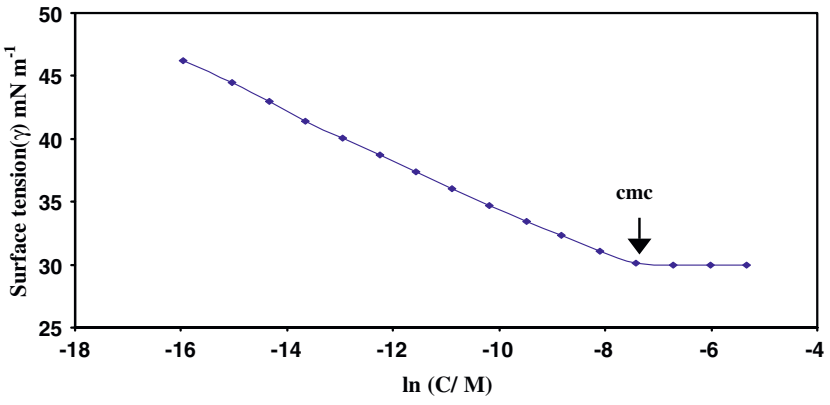

Fig. 6. Surface tension (γ) vs. ln C at different concentrations of the inhibitor (IV) at 303 K.

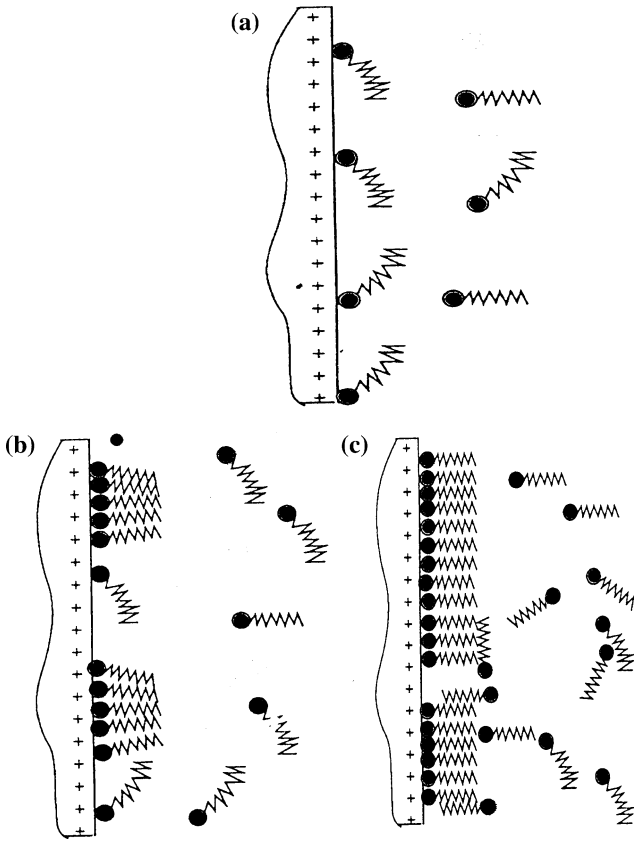

Fig. 7. Schematic representation of the inhibitor adsorption on carbon steel surface. (a) Adsorption as single molecule at low concentration. (b) Hemimicelle formation at higher concentration. (c) Formation of multi-layers at very high concentration.

surface which is directly related to the capacity of the surfactant to aggregate to form clusters (micelles). The critical micelle concentration is a key factor in determining the effectiveness of corrosion inhibition. Below the cmc as the surfactant concentration increases, the molecules tend to aggregate at the interface and this interfacial aggregation reduces surface tension. The aggregation takes place with the surfactant hydrophobic group directed towards the solvent. Micellisation is therefore a related mechanism alternative to adsorption at the interface for removing hydrophobic groups from contact with solvent , thereby reducing the free energy of the system. On the other hand, increasing the surfactant concentration above the cmc does not affect the surface tension. Above the cmc the carbon steel surface is covered with a mono layer of surfactant molecules and the additional molecules combine to form a micellar or multiple layer. This, consequently, does not alter the surface tension and corrosion rate [12].

4. Conclusions

1. The investigated ethoxylated fatty alkyl amine surfactants exhibit very good corrosion inhibition properties for carbon steel in 1 M HCl solution.

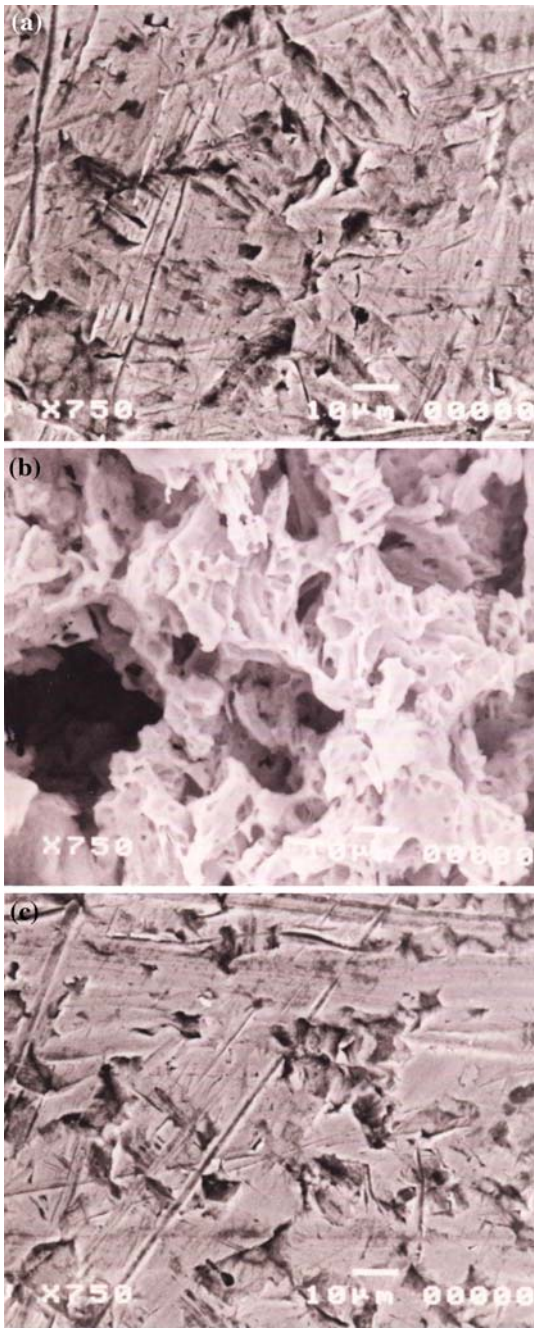

Fig. 8. Scanning electron micrographs of carbon steel samples. (a) After polishing. (b) After immersion in 1 M HCl solution for 5 days. (c) After immersion in 1 M HCl solution in presence of 400 ppm of the inhibitor for 5 days.

2. The percentage inhibition efficiency ($\eta\%$) of the compounds increases with increasing concentration until the cmc is reached.
3. The adsorption on carbon steel followed the Langmuir adsorption isotherm.
4. The potentiostatic polarisation data indicate that fatty alkyl amine surfactants act as mixed type inhibitors.
5. The percentage inhibition efficiency ($\eta\%$) increases with increasing number of ethylene oxide units and alkyl chain length.

6. The strong inhibitive properties of the surfactants is attributed to the high adsorption of the compounds on carbon steel ($K_{ads} = 1.85 \times 10^5$). This leads to the formation of a good mono layer protective film at the metal/solution interface.

References

1. L. Garverick, *Corrosion in the Petrochemical Industry* (ASM, New York, 1994).
2. A. Popova, M. Christor, S. Raicheva and E. Sokolova, *Corros. Sci.* **46** (2004) 1333.
3. M.A. Migahed, A.A. El-Safei, A.S. Fouda and M.A. Morsi, *Egypt. J. Chem.* **45** (2002) 571.
4. M.A. Migahed, H.M. Mohamed and A.M. Al-Sabagh, *Mat. Chem. Phys.* **80** (2003) 169.
5. M.A. Migahed, E.M.S. Azzam and A.M. Al-Sabagh, *Mat. Chem. Phys.* **85** (2004) 273.
6. M.A. Migahed, R.O. Aly and A.M. Al-Sabagh, *Corros. Sci.* **46** (2004) 253.
7. M.M. Osman, A.M. Omar and A.M. Al-Sabagh, *Mat. Chem. Phys.* **50** (1997) 271.
8. M.M. Osman, R.A. El-Ghazawy and A.M. Al-Sabagh, *Mat. Chem. Phys.* **80** (2003) 55.
9. Z. Abdel-Hamid, T.Y. Soror, H.A. El-Dahan and A.M. Omar, *Anti-Corros. Meth. Mat.* **45** (1998) 306.
10. G. Latha and S. Rajeswari, *Anti-Corros. Meth. Mat.* **43** (1996) 19.
11. N. Pebere, M. Duprat, F. Dabosi and A. Lattes, *J. Appl. Electrochem.* **18** (1988) 225.
12. M.L. Free, *Corros. Sci.* **44** (2002) 2865.
13. D.P. Weinsberg and V. Ashworth, *Corros. Sci.* **28** (1988) 539.
14. W. Hreczuch and A. Kozlek, *Tens. Surf. Det.* **38** (1996) 621.
15. N.D. Greene (ed.), *Experimental Electrode Kinetics* (Rensselaer Polytechnic Institute, New York, 1965).
16. K.F. Bonhoffer and K.E. Heascer, *Z. Phys. Chem. N.F.* **8** (1956) 930.
17. R. Narayan, *An introduction to Metallic Corrosion and its Prevention* (IBH publishing Co., Oxford, 1983).
18. M. Stern and A.L. Geary, *J. Electrochem. Soc.* **104** (1957) 56.
19. J.M. Abd El- Kader, A.A. El-Warraky and A.M. Abd El-Aziz, *Br. Corros. J.* **33** (1998) 139.
20. A.A. El-Shafei, S.A. Abd El-Maksoud and A.S. Fouda, *Corros. Sci.* **46** (2003) 579.
21. K.K. Al-Neami, A.K. Mohamed, I.M. Kenawy and A.S. Fouda, *Montach. Chem.* **126** (1995) 369.
22. Z.I. Osipow, *Surface Chemistry* (Reinhold publisher Co., New York, 1960).
23. H. Luo, Y.C. Guan and K.N. Han, *Corrosion* **54** (1998) 619.
24. ASTME 45-87, *Annual Book of ASTM Standard*, Vol. 11 (ASTM, Philadelphia, PA, 1980), p. 125.
25. I.L. Rozenfeld, *Corrosion Inhibitors* (New York, 1981).